Inter- and Intra-Generation Genomic Predictions for Douglas-fir Growth in Unobserved Environments

Blaise Ratcliffe[*], Francis Thistlethwaite[*], Omnia Gamal El-Dien[*,†], Eduardo P. Cappa[‡,‡‡], Ilga Porth[§], Jaroslav Klápště[**,††], Charles Chen[‡‡‡], Tongli Wang[*], Michael Stoehr[§§], Yousry A. El-Kassaby[*]

[*]Department of Forest and Conservation Sciences, Faculty of Forestry, University of British Columbia, Vancouver, BC, V6T 1Z4, Canada

[†]Pharmacognosy Department, Faculty of Pharmacy, Alexandria University, Alexandria, Egypt

[‡]Instituto Nacional de Tecnología Agropecuaria (INTA), Instituto de Recursos Biológicos, Las Cabañas y De Los Reseros s/n, 1686, Hurlingham, Buenos Aires, Argentina

[‡‡]Consejo Nacional de Investigaciones Científicas y Técnicas (CONICET), Argentina.

[§]Départment des Sciences du Bois et de la Forêt, Faculté de Foresterie, de Géographie et Géomatique, Université Laval Québec, QC, G1V 0A6, Canada

[**]Department of Genetics and Physiology of Forest Trees, Faculty of Forestry and Wood Sciences, Czech University of Life Sciences Prague, Kamycka 129, Praha 6, 165 21, Czech Republic

[††]Scion (New Zealand Forest Research Institute Ltd.), 49 Sala street, Whakarewarewa, Rotorua 3010, New Zealand

[‡‡‡]Department of Biochemistry and Molecular Biology, Oklahoma State University, Stillwater, OK 74078-3035 USA

[§§]British Columbia Ministry of Forests, Lands and Natural Resource Operations, Victoria, BC, V8W 9C2, Canada

Running title: Multi-environment single-step genomic prediction

Keywords: Bayesian mixed model, single-step GBLUP, tree improvement, genotype by environment interaction, environmental covariates, reaction norm.

Corresponding author: Yousry A. El-Kassaby
E-mail: y.el-kassaby@ubc.ca
Phone: +1 (604) 822-1821
Fax: +1 (604) 822-9106

ABSTRACT

Conifers are prime candidates for genomic selection (GS) due to their long breeding cycles. Previous studies have shown much reduced prediction accuracies (PA) of breeding values in unobserved environments, which may impede its adoption. The impact of explicit environmental heterogeneity modeling including genotype-by-environment (G×E) interaction effects using environmental covariates (EC) in a reaction-norm genomic prediction model was tested using single-step GBLUP (ssGBLUP). A three-generation coastal Douglas-fir experimental population with 14 genetic trials ($n = 13{,}615$) permitted estimation of intra- and inter-generation PA in unobserved environments using $66{,}969$ SNPs derived from exome capture. Intra- and inter-generation PAs ranged from 0.447-0.640 and 0.317-0.538, respectively. The inclusion of ECs in the prediction models explained up to 23% of the phenotypic variation for the fully specified model and resulted in the best model fit. Modeling G×E effects in the training population increased PA up to 6% and 13% over the base model for inter- and intra-generations, respectively. GS-PA can be substantially improved using ECs to explain environmental heterogeneity and G×E effects. The ssGBLUP methodology allows historical genetic trials containing non-genotyped samples to contribute in genomic prediction, and, thus, effectively boosting training population size which is a critical step. Further pheno- and enviro-typing developments may improve GS-PA.

INTRODUCTION

Breeding conifer species for phenotypic improvement is challenged due to late expression of important phenotypes related to productivity and their late sexual maturity, causing extensive recurrent selection cycles. Genomic selection (GS) can address such shortcomings through early prediction of phenotypes based on large numbers of jointly considered genomic markers, most commonly, single nucleotide polymorphisms (SNPs) (Meuwissen *et al.* 2001). This solution is realized through improved management of co-ancestry and increased genetic gain via enhanced precision and accuracy of pairwise kinship estimates for the breeding population. The recent exploration of GS within the forest tree breeding framework has produced numerous promising studies, indicating that GS prediction accuracies are able to at least match and often surpass pedigree-based predictions (see reviews by Grattapaglia 2017; Grattapaglia *et al.* 2018).

In forest trees, the effect of genotype-by-environment (G×E) interactions can be considerable and, if overlooked, detrimental to genetic gain optimization. Therefore, it is commonplace to regionalize tree breeding efforts based on available biogeoclimatic information to avoid maladaptation of deployed stock (*i.e.*, defining species' breeding zones) (Burdon 1977). However, maladaptation may still occur within regionalized areas due to trees' long lifespans, their placement within highly heterogeneous growing environments, along with ongoing and predicted shifting of climatic boundaries due to climate change. Thus, it is essential to account for the effect of G×E interactions when predicting breeding values to either select genotypes that are stable across the breeding region or match specific genotypes with particular locations to capture additional gain (Li *et al.* 2017) in the future. In forest trees' genetic evaluations, G×E interactions are typically modeled using mixed linear models that allow for covariances to be estimated between environments assuming that a character measured in two environments represents two distinct traits (*i.e.*, Type-B genetic correlations; Burdon 1977) (*e.g.* see e Silva *et al.* 2005; Cappa *et al.* 2012; Bian *et al.* 2014). However, for large numbers of environments, typically, this approach is computationally not practical and simplifications of covariance structures or factor analytic models must be put in place (Isik *et al.* 2017).

Recent GS studies in conifers have demonstrated that predictions *across* environments suffer from marked decreases in accuracy when the prediction model's training population does not include phenotypic observations from the environment to which genomic predictions were

targeted (Gamal El-Dien *et al.* 2015; Thistlethwaite *et al.* 2017; Chen *et al.* 2018). Consequently, estimated marker effects would be considered specific to the environment(s) of the training populations. Without phenotypic observations from the target environment, genomic prediction is challenging. In crop plant systems, high-dimensional environmental covariates (ECs) have been implemented in GS models to improve multi-environment genomic predictions (Jarquín *et al.* 2014). The reaction- norm models use covariance structures analogous to the realized relationship matrix (VanRaden 2008) to model environmental and G×E interaction effects. Pérez-Rodríguez *et al.* (2015) and Morais Júnior *et al.* (2018) extended the use of the reaction-norm models to include the average numerator relationship matrix (***A***) and the single-step combined relationship matrix (***H***), respectively. Pedigree-based reaction-norm methods such as random regression were only very recently proposed in a forest tree G×E interactions study (Marchal *et al.* 2019).

Single-step genomic evaluation (ssGBLUP) is a unified approach that allows the incorporation of phenotypic, genomic, and pedigree information into a single analysis (Legarra *et al.* 2009; Misztal *et al.* 2009). This methodology allows the prediction of breeding values for genotyped and non-genotyped individuals to be on the same scale, avoiding bias and complex multi-step analyses (Vitezica *et al.* 2011). It also allows for the phenotypes of non-genotyped individuals to participate in the estimation of marker effects, effectively boosting the accuracy of prediction. Thus, the method also provides a cost-effective entry into GS as relatively few important individuals can be genotyped while phenotypic records of rogued trials can also easily be implemented yielding a modern analysis for estimating marker effects or breeding values. The use of ssGBLUP has recently been demonstrated to be effective in genetic evaluations of *Picea glauca* (Ratcliffe *et al.* 2017), *Eucalyptus grandis* (Cappa *et al.* 2018), and *Eucalyptus nitens* (Klápště *et al.* 2018). However, ssGBLUP-based reaction-norm remains untested in outcrossing species such as forest trees.

A limitation of the ssGBLUP method, however, is that the combined genetic relationship matrix (***H***) can be very dense when evaluating many individuals, leading to lengthy computation times (Legarra and Ducrocq 2012). Wang *et al.* (2012a) demonstrated that genomic estimated breeding values (GEBV) of the genotyped individuals from ssGBLUP analyses can be used to calculate SNP marker effects. Lourenco *et al.* (2015) applied this approach to American Angus cattle, coining it ‘indirect prediction’. The indirect prediction approach improves computational

efficiency and allows for fast prediction of GEBV for new genotyped trees via SNP marker effects as opposed to a full ssGBLUP evaluation where new genotyped individuals need to be explicitly included.

This study is based on the 'maritime low' coastal Douglas-fir (CDF) (*Pseudotsuga menziesii* (*Mirb.*) Franco var. *menziesii*) seed planning unit (SPU) which represents elevation bands 0-900m in geographic areas west of the British Columbia (BC) coastal mountain range and latitudinal gradients South 48°00' - 52°00'. The CDF breeding program is the most advanced in BC and is currently in its third generation with advanced generation seed orchards producing 6.6 million seedling equivalents from 2012 to 2017. Using 14 experimental trials planted in different environments, we used monthly averages of ECs obtained from ClimateBC (Wang *et al.* 2012b), and ssGBLUP (Legarra *et al.* 2009; Misztal *et al.* 2009) under a Bayesian mixed-model framework (Pérez and de los Campos 2014) to obtain genetic parameter estimates and genomic estimated breeding values for genotyped individuals. We then used the method of Lourenco *et al.* (2015) to obtain indirect predictions of breeding values of target populations in unobserved environments. Thus, the objectives of this study were to assess the influence of including monthly average ECs for environment and G×E effects in mixed model analysis on i) genetic parameter estimates for the studied population, ii) model fit criteria, and iii) between-environment genomic prediction accuracies for intra- and inter-generational predictions.

MATERIALS AND METHODS

Study populations

Study population 1 (SP1)

The trees in this study are from low elevation (0-900m asl), third generation coastal Douglas-fir (*Pseudotsuga menziesii* (Mirb.) Franco var. *menziesii*) breeding population located in coastal British Columbia, Canada (Table 1). The parental (P0) generation consists of 78 wild plus-tree selections, which were crossed in partial disconnected diallels to produce 165 full-sib families for the second generation (F1). Full-sib families of the second generation were planted in 1975 using nursery container stock in ten environments using randomized complete block designs with four replicates per environment and four tree family row plots within the replicates (mean ≈ 15; range = 14-16; trees / full-sib family / environment). The third generation (F2) contains two series (F2-2, F2-3), with no common parentage between them (see Figure S1,Table S1, Table S2) and are the result of crossing forward selections from the F1 generation, based on tree volume. F2-2 and F2-3 were planted in 2003 and 2006 respectively, both using nursery container stock, and both planted as full-sib block tests with 5 × 5 tree plots on two environments per series (mean ≈ 19; range ≈ 17-21; trees / full-sib family / environment). A total of 31,999 tree height [cm] phenotypic measurements were available for ages 12 (F1) and 11 (F2-2 and F2-3). Phenotypes were standardized by dividing total tree height by age [years] at time of measurement to provide the mean annual increment (MAI [cm]).

Study population 2 (SP2)

A subset of SP1 was used for the genomic analyses in this study (Table 2). The subset population was created by setting a relatedness threshold of greater than 0 as the minimum expected additive genetic kinship coefficient value (***A***, derived via pedigree) of an individual tree in the F1 or F2 generations, with at least one of the genotyped individuals in the F2 population. This resulted in 11,759 F1 phenotypes available for the genomic analyses (mean ≈ 15; range ≈ 14-16;

trees / full-sib family / environment). The relatedness restriction resulted in an average additive genetic kinship coefficient of 0.033, as opposed to 0.012 in the population described previously.

SNP genotyping

SNP genotypes were based on those produced and used by Thistlethwaite *et al.* (2017, 2019) with the full details available in Thistlethwaite *et al.* (2017). Briefly, DNA was extracted from cambial tissue and sent to RAPiD Genomics© (Florida, US) for SNP genotyping using whole exome capture. The SNPs used here differed from those used by Thistlethwaite *et al.* (2017, 2019) due to filtering criteria resulting in a different number of SNPs and genotyped trees for this study. Filtering criteria was done using VCFtools (Danecek *et al.* 2011) and were as follows: maximum number of alleles = 2, minimum number of alleles = 2, Hardy-Weinberg Equilibrium exact test = 0.10, maximum sample missing = 0.40, maximumSNP missing = 0.40, minor allele frequency = 0.05, maximum site read depth = 50, minimum site read depth = 4. We then used the 'impute.svd' function from the R package 'bcv' (Perry 2015) to impute the remaining missing data resulting in a final count of 66,969 SNPs for the genomic analyses.

Environmental covariates (ECs)

Thirteen monthly ECs were obtained using ClimateBC software version 5.51 (Wang *et al.* 2012b) resulting in 156 individual environmental covariates per environment (*i.e.*, 12 months by 13 variables). ClimateBC generates "scale-free" climate data, thus allows the user to obtain monthly climate variables for specific test environments rather than pixel averages from grid-based climate data. Monthly ECs were averaged across the growing period for each trial, from planting year until the year of phenotypic measurement, and included primary measures of temperature, precipitation, and solar radiation (see Table S3 for a complete list of the thirteen primary and derived monthly variables).

Pedigree-based analyses (PBLUP)

PBLUP analyses were used to estimate (co)variance components or functions of them (*i.e.*, heritabilities and Type-B genetic correlations) and breeding values for the experimental population outlined in Table 1. All PBLUP analyses were completed using ASReml-R v3.0 (Butler *et al.* 2009), which uses the Average Information algorithm on Restricted Maximum Likelihood (REML) (Gilmour *et al.* 1995).

Individual-tree breeding values were obtained under the following multi-environmental mixed linear model:

$$\boldsymbol{y} = \boldsymbol{X\beta} + \boldsymbol{Z_r r} + \boldsymbol{Z_f f} + \boldsymbol{Z_a a} + \boldsymbol{e} \quad [1]$$

where $\boldsymbol{y}$ is the vector of phenotypic observations; $\boldsymbol{\beta}$ is the fixed effect of environment means; $\boldsymbol{r}$ is the vector of random replicate effects within of each F1 environment, with $\boldsymbol{r} \sim \boldsymbol{N}(\boldsymbol{0}, \boldsymbol{G_r} \otimes \boldsymbol{I})$, where $\boldsymbol{G_r}$ is the diagonal (co)variance matrix between environments with diagonal elements $\sigma^2_{r_i}$ for each environment i representing the replicate within environment variances, $\boldsymbol{I}$ is the identity matrix, and $\otimes$ represents the Kronecker product of matrices; $\boldsymbol{f}$ is the vector of random full-sib family genetic effects, with $\boldsymbol{f} \sim \boldsymbol{N}(\boldsymbol{0}, \boldsymbol{G_f} \otimes \boldsymbol{I})$, where $\boldsymbol{G_f}$ is the diagonal dominance (co)variance matrix between environments with diagonal elements σ^2_f representing ¼ of dominance genetic variance (*i.e.*, a common family variance for all environments was used); $\boldsymbol{a}$ is the vector of additive genetic effects (or breeding values, EBV), with $\boldsymbol{a} \sim \boldsymbol{N}(\boldsymbol{0}, \boldsymbol{G_a} \otimes \boldsymbol{A})$ where $\boldsymbol{G_a}$ is the additive genetic (co)variance matrix between environments with diagonal elements σ^2_a representing additive genetic variance and off-diagonal elements σ_a (*i.e.*, a common additive genetic variance and covariance for all environments was used) representing the same additive genetic covariance between environments, and the matrix $\boldsymbol{A}$ contains the additive genetic relationships among all trees; $\boldsymbol{X}$, $\boldsymbol{Z_r}$, $\boldsymbol{Z_f}$, and $\boldsymbol{Z_a}$ are the respective incidence matrices assigning fixed and random effects to each observation. Finally, $\boldsymbol{e}$ is the vector of random residual effects, with $\boldsymbol{e} \sim \boldsymbol{N}(\boldsymbol{0}, \boldsymbol{R})$, where $\boldsymbol{R} = \oplus \boldsymbol{I}\, \sigma^2_{e_i}$, $\sigma^2_{e_i}$ is the residual variance for each environment i, and $\oplus$ represents the 'direct sum' of matrices. We chose to use a common variance for genetic dominance and additive effects to allow a more parsimonious model when using a large number of trees and environments.

Single-environment narrow-sense heritability for each environment i (h_i^2) was calculated using the same model from Eq. [1], except that in $\boldsymbol{G_a}$ different σ_a^2 were used for each environment i ($\sigma_{a_i}^2$) (*i.e.*, CORUH structure in ASReml). Then, h_i^2 were estimated as: $h_i^2 = \sigma_{a_i}^2/(\sigma_{a_i}^2 + \sigma_f^2 + \sigma_{e_i}^2)$.

Finally, pairwise Type-B genetic correlations between environments i and i' ($r_{g_{ii'}}$) were estimated using the model of Eq. [1] but fitting two environments at the time, and $\boldsymbol{G_a}$ was a heterogeneous (co)variance matrix with different additive genetic variances among environments and an additive genetic covariance between pairs of environments i and i' equal to $\sigma_{a_{ii'}}$ (*i.e.*, US structure in ASReml) was used for the vector random additive genetic effects in this case. For this analysis, only two environments were fitted to the model at a time. Then, $r_{g_{ii'}}$ was estimated as: $r_{g_{ii'}} = \sigma_{a_{ii'}}/\sqrt{\sigma_{ii}^2\sigma_{i'i'}^2}$.

Genomic-based analyses (ssGBLUP)

Variance components, genetic parameters, and model fit (Deviance Information Criterion, Spiegelhalter *et al.* 2002) were estimated by fitting models to the data set in Table 2. Following Jarquín *et al.* (2014), the models fit were a series of five linear hierarchical single-step GBLUP (ssGBLUP) models. The R package 'BGLR' (Pérez and de los Campos 2014) was used. For variance component estimation, all data in Table 2 was fit to each model and the Monte Carlo Markov Chain (MCMC) was generated with 200,000 iterations thinned at a rate of 5, with the first 25,000 discarded as burn-in. Bayesian ridge regression (BRR; Gaussian prior) model was used for all model effects. The 'BGLR' package default starting parameters were used. Multiple chains were generated and the MCMC chain posterior means and trace plots of the posterior distributions were compared to confirm convergence. Cholesky decomposition of all variance-covariance matrices was used to speed up computations.

Model 1 (M1):

The first ssGBLUP model included an overall mean (μ) as a fixed effect, random environment effects ($\boldsymbol{S_i}$), random replicate ($\boldsymbol{R_k}$), and random additive genetic effects ($\boldsymbol{a_j}$). Let $\boldsymbol{y_{ijk}}$ and $\boldsymbol{e_{ijk}}$ be

the phenotype and residual effects, respectively, of individual j for environment i, scored in replicate k. Then the mixed model to analyze the data is:

$$\boldsymbol{y_{ijk}} = \mu + \boldsymbol{S_i} + \boldsymbol{R_k} + \boldsymbol{a_j} + \boldsymbol{e_{ijk}} \quad [2]$$

where $\boldsymbol{S_i} \sim \boldsymbol{N}(\boldsymbol{0}, \boldsymbol{I}\sigma_s^2)$, $\boldsymbol{R_k} \sim \boldsymbol{N}(\boldsymbol{0}, \boldsymbol{I}\sigma_r^2)$, $\boldsymbol{a_j} \sim \boldsymbol{N}(\boldsymbol{0}, \boldsymbol{H}\sigma_a^2)$, and $\boldsymbol{e_{ijk}} \sim \boldsymbol{N}(\boldsymbol{0}, \boldsymbol{I}\sigma_e^2)$ where the respective variances σ_s^2, σ_r^2, σ_a^2, and σ_e^2 are common for all the environments. The combined additive genetic relationship matrix, $\boldsymbol{H}$, was calculated as follows (Legarra *et al.* 2009; Christensen and Lund 2010):

$$\boldsymbol{H} = \begin{bmatrix} \boldsymbol{A}_{11} + \boldsymbol{A}_{12}\boldsymbol{A}_{22}^{-1}(\boldsymbol{G} - \boldsymbol{A}_{22})\boldsymbol{A}_{22}^{-1}\boldsymbol{A}_{21} & \boldsymbol{A}_{12}\boldsymbol{A}_{22}^{-1}\boldsymbol{G} \\ \boldsymbol{G}\boldsymbol{A}_{22}^{-1}\boldsymbol{A}_{21} & \boldsymbol{G} \end{bmatrix}$$

where $\boldsymbol{A}_{11}$ is the portion of the average numerator relationship matrix ($\boldsymbol{A}$) including the non-genotyped individuals, $\boldsymbol{A}_{22}$ is the portion of genotyped individuals, and $\boldsymbol{A}_{12}$ and $\boldsymbol{A}_{21}$ are the portions containing the expected additive genetic relationships between genotyped and non-genotyped individuals. The genomic additive relationship matrix for genotyped individuals, $\boldsymbol{G}$, was calculated after VanRaden (2008):

$$\boldsymbol{G} = \boldsymbol{M}\boldsymbol{M}'/\Sigma_l p_l(1 - p_l)$$

where $\boldsymbol{M}$ is the centered matrix of SNP covariates, and p_l is the current (or observed) allele frequency of the genotyped trees for marker l. Further, $\boldsymbol{G}$ was scaled for compatibility with $\boldsymbol{A}$ such that the mean diagonal and off-diagonal elements were equal (Christensen *et al.* 2012):

$$\boldsymbol{G}^* = \beta\boldsymbol{G} + \alpha,$$
$$\begin{cases} Avg(diag(\boldsymbol{G}))\beta + \alpha = Avg(diag(\boldsymbol{A}_{22})) \\ Avg(\boldsymbol{G})\beta + \alpha = Avg(\boldsymbol{A}_{22}) \end{cases}$$

To avoid potential problems with the inversion of $\boldsymbol{G}^*$, it was weighted as (Aguilar *et al.* 2010):

$$\boldsymbol{G_w} = 0.95 \times \boldsymbol{G}^* + (1 - 0.95) \times \boldsymbol{A}_{22} \quad [8]$$

Model 2 (M2):

$$\boldsymbol{y_{ijk}} = \mu + \boldsymbol{S_i} + \boldsymbol{R_k} + \boldsymbol{a_j} + \boldsymbol{w_{ij}} + \boldsymbol{e_{ijk}} \quad [3]$$

M2 extends model M1 (Eq. [2]) to include the vector of random effects for environmental covariates ($\boldsymbol{w}$) which is distributed as $\boldsymbol{w} \sim \boldsymbol{N}(\boldsymbol{0}, \boldsymbol{\Omega}\sigma_w^2)$. Where $\boldsymbol{\Omega}$ is the matrix of similarity among environments calculated as $\boldsymbol{\Omega} \propto \boldsymbol{WW'}/q$, with $\boldsymbol{W}$ being a centred and standardized matrix of ECs and q the number of ECs as described by (Jarquín *et al*. 2014) in detail, and σ_w^2 is the variance of the vector of ECs.

Model 3 (M3):

$$\boldsymbol{y_{ijk}} = \mu + \boldsymbol{S_i} + \boldsymbol{R_k} + \boldsymbol{a_j} + \boldsymbol{w_{ij}} + \boldsymbol{aw_{ij}} + \boldsymbol{e_{ijk}} \quad [4]$$

M3 incorporates the vector of random effects for the interaction between additive genetic ($\boldsymbol{a}$) and EC ($\boldsymbol{aw}$), $\boldsymbol{aw} \sim \boldsymbol{N}(\boldsymbol{0}, \boldsymbol{Z_a HZ'_a} \circ \boldsymbol{\Omega}\sigma_{aw}^2)$, where σ_{aw}^2 is the variance of the interaction between additive genetic effects and ECs, and ∘ is the Hadamard (Schur) product of matrices.

Model 4 (M4):

$$\boldsymbol{y_{ijk}} = \mu + \boldsymbol{S_i} + \boldsymbol{R_k} + \boldsymbol{a_j} + \boldsymbol{w_{ij}} + \boldsymbol{aS_{ij}} + \boldsymbol{e_{ijk}} \quad [5]$$

M4 includes a vector of random effects for the interaction between additive genetic and main environment terms ($\boldsymbol{aS}$), $\boldsymbol{aS} \sim \boldsymbol{N}[\boldsymbol{0}, \boldsymbol{Z_a HZ'_a} \circ (\boldsymbol{Z_S Z'_S})\sigma_{aS}^2]$, where $\boldsymbol{Z_S}$ is the incidence matrix for the effects of environments, and $\boldsymbol{\sigma_{aS}^2}$ is the variance of the interaction between additive genetic and main environmental effects.

Model 5 (M5):

$$\boldsymbol{y_{ijk}} = \mu + \boldsymbol{S_i} + \boldsymbol{R_k} + \boldsymbol{a_j} + \boldsymbol{w_{ij}} + \boldsymbol{aw_{ij}} + \boldsymbol{aS_{ij}} + \boldsymbol{e_{ijk}} \quad [6]$$

Finally, M5 includes both interaction effects from M3 (*i.e.*, $\boldsymbol{aw}$) (Eq. [4]) and M4 (*i.e.*, $\boldsymbol{aS}$) (Eq. [5]).

Prediction accuracy and cross-validation

Two scenarios were considered for estimating the prediction accuracy of the validation populations (VP, Table 2). In the first scenario (GA1), a leave one environment out approach for environments with genotyped individuals (Lost, Adam, and Fleet) was used to form the training population (TP). In the second scenario (GA2), the TP consisted of all individuals from the F1 generation. In either case, the non-genotyped individuals of the TP were randomly divided into five folds, that is, the phenotypes of genotyped individuals in the TP always participated in the estimation of SNP marker effects. The random folding process was replicated three times for each model (M1-M5). For each fold, genomic estimated breeding values (GEBV) of the genotyped VP were correlated to their EBV estimated in the PBLUP analysis (Eq. [1]). Prediction accuracy ($r_{(GEBV,EBV)}$) was then calculated as the mean Pearson product-moment correlation of the three replicates. The procedure for obtaining GEBV for the VP follow closely the methods of Lourenco *et al.* (2015) and are outlined below.

Estimation of GEBV for the validation population

1) Use ssGBLUP models M1-M5 to obtain the vector of GEBV ($\boldsymbol{a}$) for the genotyped portion of the TP.
2) Calculate the direct genomic value for each genotyped tree j (DGV_j) in the TP (Aguilar et al. 2010):

$$DGV_j = -\left(\sum_{j',j'\neq j} g^{j'j} GEBV^{j'} / g^{jj}\right)$$

where $g^{j'j}$ (and g^{jj}) is an off-diagonal (and diagonal) element of the inverse of $\boldsymbol{G}$ ($\boldsymbol{G^{-1}}$) corresponding to relationships between tree j' and j and $GEBV^{j'}$ is the predicted additive genetic solutions from the ssGBLUP models M1-M5 for TP and individual j'.

3) Estimate SNP marker effects from the TP:

$$\hat{\boldsymbol{u}} = \boldsymbol{D}\boldsymbol{M}'\boldsymbol{G}^{-1}(\boldsymbol{D}\boldsymbol{G}\boldsymbol{V})$$

where $\hat{\boldsymbol{u}}$ is the vector of estimated SNP effects, $\boldsymbol{D}$ is a weight diagonal matrix for SNP (here an identity matrix), $\boldsymbol{M}$ as defined before, and DGV is the vector of DGV for the TP.

4) Calculate DGV for the trees in the VP:

$$DGV_j = \boldsymbol{M}_j\hat{\boldsymbol{u}}$$

where DGV_j and $\boldsymbol{M}_j$ are the direct genomic values and the matrix of centered genotypes for tree j in the VP and not included in the ssGBLUP models M1-M5, respectively.

5) Calculate GEBV for the VP:

$$GEBV_j \approx w_1 PA + w_2 DGV_j \quad [16]$$

where PA is the parental average of individual j in the VP and w_1 and w_2 are weights associated with the covariances of DGV_j and PA:

$$\begin{bmatrix} w_1 \\ w_2 \end{bmatrix} = \begin{bmatrix} \sigma^2_{PA} & \sigma_{PA,DGV_j} \\ \sigma_{DGV_j,PA} & \sigma^2_{DGV_j} \end{bmatrix} \begin{bmatrix} \sigma^2_{PA} \\ \sigma^2_{DGV_j} \end{bmatrix}$$

Lourenco *et al.* (2015) note that this approximation excludes the pedigree prediction component from the selection index approach proposed by VanRaden *et al.* (2009). Parental breeding values for the F1 generation were calculated as the average breeding value of all offspring without masked phenotypes. Parental breeding values for the F2 generation were directly estimated in the prediction models.

Data availability

All statistical analyses were carried out in the R environment (R Core Team 2017). Phenotypic and genotypic data are available from the Dryad Digital Repository https://doi.org/10.5061/dryad.8n2d374.

RESULTS

Pedigree-based analyses (PBLUP)

Individual tree single environment narrow-sense heritability estimates for the PBLUP analysis were low to moderate for the F1 generation trials ($\hat{h}_i^2 = 0.04 - 0.27$) while estimates for the F2 generation were higher ($\hat{h}_i^2 = 0.13 - 0.42$) (Table 3). Standard errors of heritability estimates were low indicating significance of the estimates. Type-B genetic correlation estimates between F1 trials were positive and generally high ($\hat{r}_{g_{ii'}} = 0.51 - 0.98$), representing agreement in allelic effects contributing to MAI among the tested environments. This result is expected since the trials are from a single breeding zone. Among the three genotyped F1 trials (Lost, Adam, Fleet) the Type-B genetic correlations were moderate to high ($\hat{r}_{g_{ii'}} = 0.71 - 0.88$), and between environments of F2-2 ($\hat{r}_{g_{ii'}} = 0.62$) and F2-3 ($\hat{r}_{g_{ii'}} = 0.57$). Type-B genetic correlations between F1 and F2 trials were in most cases not significant based on standard errors or were non-estimable due to low genetic connectivity between environments (see Figure S1, Table S1, Table S2).

Genomic-based analyses (ssGBLUP)

In M1 46% and 5% of the phenotypic variance was explained by the between environment ($\hat{\sigma}_S^2$) and within environment ($\hat{\sigma}_r^2$) effects, respectively (Table 4). With the addition of ECs ($\hat{\sigma}_w^2$) in M2 those values dropped to 34% and 3% respectively, with the ECs accounting for 22% of the phenotypic variance. The shift of explained variance from the between environment effect to ECs can be understood as a decomposition of environmental variance, showing that ECs in M2 are able to capture additional environmental variation not captured by M1. This shift was accompanied by 9% decrease in error variance ($\hat{\sigma}_e^2$) across models M1-M5. However, a minor increase in the DIC model fit statistic of M2 did not justify the addition of ECs to M1.

Evaluating the addition of G×E interactions into the model structure (M3-M4) showed that the use of ECs ($\hat{\sigma}_{aw}^2$) in M3 explained 4% more phenotypic variation than the use of the environment interaction effect ($\hat{\sigma}_{aS}^2$) in M4. Large decreases in the DIC model fit statistic were observed with the addition of either $\boldsymbol{aS_{ij}}$ or $\boldsymbol{aw_{ij}}$ interaction effects in the model, justifying their

use; however, when considering them individually the $\boldsymbol{aw_{ij}}$ effect offered a better DIC model fit statistic. The joint use of both $\boldsymbol{aS_{ij}}$ and $\boldsymbol{aw_{ij}}$ interaction effects in the model to explain G×E accounted for 9% of the total phenotypic variation, indicating a small but important source of genetic variation in the breeding population. The DIC estimate for the most complex model (M5) was lowest, justifying the specification and use of all model parameters for the prediction of breeding values in this population.

Narrow-sense heritability estimates for models M1-M5 were in agreement with the mean single environment narrow-sense heritability estimates from the prior PBLUP analysis. A decrease in additive genetic variance estimates and consequently narrow-sense heritability, was observed with increasing model complexity due primarily to the addition of G×E effects into the models, and a decrease in percent variance explained by the additive genetic effect ($\hat{\sigma}_a^2$) 9% M1 vs 7% M2-M5. The decrease in heritability highlights the confounding nature between additive genetic effect estimates and G×E interaction effects.

Genomic prediction accuracy

Intra-generation (GA1)

Models M1-M5 prediction accuracies for EBV of genotyped individuals across environments and within the F1 generation varied ($r_{(GEBV,EBV)} = 0.447 - 0.640$) (Table 5, Figure 1). Individual environment mean prediction accuracies for models M1-M5 were not equal among the three tested environments $r_{(GEBV,EBV)} = 0.619$ (Lost), $r_{(GEBV,EBV)} = 0.513$ (Fleet), and $r_{(GEBV,EBV)} = 0.452$ (Adam). The addition of ECs facilitated by model M2 gave minor increases in prediction accuracy, up to 2% over M1 (Fleet). Gains in prediction accuracy of up to 6% (M3, Lost; M5, Fleet) were observed by accounting for G×E effects in the population. Treatment of G×E effects using ECs (M3) performed better than using main environment effects (M4) when comparing to the base model scenario (M2). Standard errors of predictions were minor, ranging from 0.0000-0.0027, indicating low variation between cross-validation replicates.

Inter-generation (GA2)

Testing the models to predict EBV across generations and across environments yielded an expectedly lower minimum prediction accuracy than observed for GA1 ($r_{(GEBV,EBV)} = 0.317 -$

0.538) (Table 6, Figure 1). In all models, prediction accuracies were greater for the Bigtree environment than they were for Jordan. Comparison of models M1 and M2 show that the addition of ECs in M2 did not produce an increase in prediction accuracy for Bigtree and a 1% decrease was observed for Jordan. The addition of individual G×E terms in models M3 and M4 both gave increases in prediction accuracy over the base model M1 for both Jordan and Bigtree. However, the use of ECs to explain G×E variation (M3) gave 13% (Jordan) and 6% (Bigtree) increases in prediction accuracies over M1 versus 8% (Jordan) and 4% (Bigtree) given by M4. No improvement in prediction accuracy occurred for Jordan with the addition of both G×E terms in model M5 and estimates were, in fact, equal to those given by M3. For the Bigtree environment, a small 2% gain in prediction accuracy was observed for model M5 over model M4 versus 1% for model M3.

DISCUSSION

The capability of GS and its application to increase genetic gain in conifer forest tree breeding programs is at this point recognized as being a future certainty (Grattapaglia *et al.* 2018). Genetic gain is ultimately a product of trait heritability, accuracy, and intensity of selection, and the time interval to complete a round of selection, testing, and breeding. Of these factors, the accuracy of selection and time effort are most effectively addressed by GS methods. Previously, with forest trees, the ssGBLUP method was demonstrated by Ratcliffe *et al.* (2017), Cappa *et al.* (2018) and Klápště *et al.* (2018) to improve the accuracy of genetic parameter estimates and intra-generation breeding values in forest trees. Here, the ssGBLUP methodology permitted the use of rogued genetic trial data by collectively leveraging their phenotypic, pedigree and genomic information to participate in marker effect estimation and subsequent intra- and inter-generation breeding value predictions. Additionally, the merit of using indirect genomic predictions with the ssGBLUP method was supported by this study in reducing the computational time required to obtain predictions for unobserved samples.

We further demonstrated the capabilities of ssGBLUP in boosting (or increasing) the training population size without the need of extra genotyping, an important aspect of genomic prediction accuracy highlighted by Hayes et al. (2009). As a result, the training population ($n = 11{,}759$) used here, so far represents the largest for a genomic prediction study in forest trees. A study involving Norway spruce highlighted that a TP to VP ratio of up to 3:1 produced increased prediction accuracies for growth and wood quality traits (Chen *et al.* 2018). However, it should be noted that Tan et al. (2017) and Lenz et al. (2017) observed benefit in prediction accuracy above the stated 3:1 ratio. Training population size is critical when the G×E effect can be as substantial as commonly observed in forest trees. Thus, it is a boon when historical trials which represent testing of genotypes across many environments can be recovered and included in the genomic prediction analysis. Additionally, larger training populations will better capture trait architecture and the totality of genetic diversity of the breeding population, a substantial benefit for making inferences. This variation may include rare marker variants, which are effective for the prediction of oligogenic traits where they may account for larger proportions of trait heritability (*e.g.*, Resende *et al.* 2017). In our analysis, the studied trait (MAI) is considered to have low heritability and complex genetic architecture (*i.e.*, polygenic). Indeed, the heritability

estimates (Table 3, Table 4) and marker effect plot (Figure S2) agree, justifying the use of the BRR model and Gaussian prior choice for prediction of the GEBV.

We investigated the effect of modeling G×E interactions on GS prediction accuracies in Douglas-fir, an outcrossing conifer tree species. Thereby, we demonstrated increased inter- and intra-generation prediction accuracy of EBV through consideration of G×E effects defined not only by main environment effects but also by ECs in the predictive models. The inclusion of EC effects in the model by themselves (*i.e.*, M2) presented a fractioning of the phenotypic variance into effects explained by the main environment effect (34%) and that of the ECs (22%). This was accompanied by a 7% decrease in the proportion of total variance explained by the residual effect, thus producing more realistic gain estimates. However, in most cases M2 offered little to no increase in prediction accuracy over M1, which agrees with the results of previous studies which tested the same suite of models used here for various traits in plants such as rice, wheat, or cotton (Jarquín *et al.* 2014; Pérez-Rodríguez *et al.* 2015; Morais Júnior *et al.* 2018). Jointly, the specification of EC effects, $\boldsymbol{w_{ij}}$ and $\boldsymbol{aw_{ij}}$, in M3 resulted in a decrease in estimated residual variance over M1 (16%) and the interaction effect explained 9% of the phenotypic variation versus 5% of $\boldsymbol{aS_{ij}}$, the interaction specified using the main environment effect (M4). Additionally, models M3 and M5 showed the most consistent increases in prediction accuracy over the base model M1 which also corroborates the aforementioned crop plant-based studies.

In our analysis, maximum intra-generation prediction accuracies were achieved using either M3 or M5 which always included $\boldsymbol{w_{ij}}$ and $\boldsymbol{aw_{ij}}$ and ranged from $r = 0.461 - 0.640$ depending on the target environment, which are similar to previous reports of intra-generation GS prediction accuracies based on multi-environment trials using conifer trees. Though many previous studies did not explicitly model or test the inclusion of G×E interaction effects in the training population or GS prediction model. For example, and perhaps most informative, was a four environment GS analysis of loblolly pine (*Pinus taeda*) by Resende *et al.* (2012) which showed an average decrease of 23% in prediction accuracies for tree height (age 6) when the prediction was done in unobserved environments within the same breeding zone ($r = 0.41 - 0.74$). However, the same study noted an average decrease of 41% when the prediction was extended to between breeding zones ($r = 0.23 - 0.55$). Thus, Resende *et al.* (2012) stressed the importance of regionalizing tree breeding efforts, breeding zone delineation, and the lack of transferability of genomic prediction models across breeding zones. A later study by Beaulieu *et*

al. (2014) found large decreases (33-41%) in prediction accuracies for Quebec white spruce (*Picea glauca*) tree height (age 17) when predicting EBV in unobserved environments ($r = 0.22 - 0.34$). Lenz (2017) however, reported only 2% and 9% reductions in prediction accuracy for 25 year tree height for black spruce (*Picea mariana*) when their prediction model did not include the target environment ($r = 0.52 - 0.56$). The results observed by Lenz *et al.* (2017) reflect the low G×E effects of their black spruce population.

Two previous studies did however explicitly model GxE in the training population. The first by Gamal El-Dien *et al.* (2015) showed an average decrease of 29% in genomic prediction accuracy of tree height (age 38) for interior spruce (*Picea glauca* × *engelmannii*) when the target environment was not explicitly included in the training population ($r = 0.37 - 0.53$). However, the mentioned study did not compare the inclusion of specific model terms for G×E to investigate their impact on prediction accuracy as was done in the present study. The second by Thistlethwaite *et al.* (2017) was based on the same F1 population of trees studied here, albeit with differences (see further discussion). Thistlethwaite *et al.* (2017) observed prediction accuracies of $r = 0.88 - 0.93$ for age 12 tree height. This result contrasts with previous studies, since it is higher than the average prediction accuracy when the training population contained observations from all three environments ($r = 0.88$).

Empirical studies examining inter-generation GS prediction accuracies in forest tree species are very limited. Isik *et al.* (2016) were the first to include multiple generations in a genomic selection analysis of a forest tree. The prior study was continued by Bartholomé *et al.* (2016) who observed moderately high prediction accuracies ($r = 0.70$) for age 12 tree height when using a training population of grandparents and parents to predict offspring. Using samples from the same breeding population of this study, Thistlethwaite *et al.* (2019) observed inter-generation prediction accuracy of $r = 0.42$ for the Jordan environment. However, the results presented by Thistlethwaite *et al.* (2019) are not directly comparable to those presented here due to many key methodological differences: i) genomic prediction methods, ii) training and validation population structure and composition, iii) marker subset and imputation method, iv) estimation method of EBV, and v) modeling of G×E factors. The inter-generation prediction accuracies observed in this study were nevertheless lower than those of the study for maritime pine juvenile tree height ($r = 0.70$) (Bartholomé *et al.* 2016). Maximum inter-generation

prediction accuracies for MAI here were $r = 0.360$ (Jordan) and $r_{(GEBV,EBV)} = 0.538$ (Bigtree) given by model M6 in both cases.

The inclusion of a main G×E interaction term is standard in individual-tree mixed models, yet the inclusion of ECs to explain environmental heterogeneity and genetic variation is not yet widely used in forestry. With the availability of 'scale-free' climate data for specific locations from programs such as ClimateBC (Wang *et al.* 2012b) and the NASA POWER Project (Stackhouse *et al.* 2017), breeders should opt for their use to help describe growing conditions and improve EBV predictions. Type-B genetic correlations in this study were high between the predicted F1 environments ($\hat{r}_{g_{ii'}} = 0.71 - 0.88$), which might account for the moderately high intra-generation prediction accuracies observed here. However, Coastal Douglas-fir is noted to have strong G×E interaction for growth traits (Campbell 1992; Cappa *et al.* 2016), which may also help to explain the observed gain in prediction accuracy in this study by accounting for G×E effects. Thus, it appears to be critical for species with moderate to strong G×E interactions to either i) explicitly include the target environment in the GS prediction model, or ii) incorporate G×E effects in the genomic prediction model by including observations from as many environments as possible from across the breeding zone, an opportunity made possible with ssGBLUP.

To our knowledge, this is the first use of ECs to capture environmental heterogeneity and G×E effects on phenotypic variation in outcrossing trees for genomic prediction of breeding values. The prior mentioned studies concerning forest trees and multi-environment trials have not considered methods to improve predictions in unobserved environments as was done in this study. Here, we advocate the inclusion of $\boldsymbol{w_{ij}}$, as well as both $\boldsymbol{aS_{ij}}$ and $\boldsymbol{aw_{ij}}$ interaction effects in the model as the gain in prediction accuracy was generally consistent across all tested environments and generations.

From a practical standpoint, the base (M2) and fully specified (M5) models were mostly agreeable in candidate rankings of the predicted individuals from unobserved environment (Figure S3). It is clear from the low discordance in rankings of highest and lowest ranked individuals that the same selections would be made irrespective of the model used. However, forest tree breeding programs by necessity require minimum effective population sizes (N_e) which requires the selection of some sub-optimal individuals to maintain adequate genetic diversity in the breeding population. For these individuals (*i.e.*, mid-ranked candidates) there is

much less concordance in rankings between the two models. During this phase the selection of these individuals becomes important to balance genetic gain with and genetic diversity in the breeding population. This result is in agreement with Stejskal et al. (2018) who noted the capacity of GS to accurately capture Mendelian sampling (*i.e.*, within family genetic variance) and cryptic relatedness in the breeding population, making it a preferred approach over traditional pedigree-based selection in forestry.

In addition to the combination of high-density genomic and environmental/climate data, it is realistic to assume that prediction of phenotypes can be further improved through the simultaneous inclusion of multiple phenotypic and environmental traits obtained via high-throughput platforms such as those produced by remote sensing (Araus *et al.* 2018; Dungey *et al.* 2018). Information sharing between genetic lines, correlated traits and correlated environments via multiple-trait models with the specification of G×E interaction effects will lead to improved phenotypic predictions. Finally, as the anticipated increasing role of GS in tree breeding, it is essential to highlight the importance of prediction accuracy improvement through the utilization of all possible available information such as was demonstrated here with the inclusion of non-genotyped individuals and their testing environments, as well as environmental covariates to better model G×E effects.

ACKNOWLEDGEMENTS

The authors would like to thank Odilon Peixoto de Morais Júnior for their help with the statistical analysis.

This work was supported by Genome British Columbia (User Partnership Program (UPP-001) to YEK and MS, NSERC Discovery Grant to YEK, TimberWest Forest Corp., and Western Forest Products Inc. We declare that the funding agencies did not participate in the design of the study and collection, analysis, and interpretation of data and in writing the manuscript.

AUTHOR CONTRIBUTIONS

BR, YEK, and MS conceived the study. BR, EPC, and FT performed the data analysis. MS, IP, FT for phenotypic data collection and DNA extraction. BR drafted the manuscript. CC, EPC, OG, IP, TW, JK, MS, YEK, and FT provided instrumental comments, feedback, and technical support.

REFERENCES

Aguilar I., I. Misztal, D. L. Johnson, A. Legarra, S. Tsuruta, *et al.*, 2010 Hot topic: A unified approach to utilize phenotypic, full pedigree, and genomic information for genetic evaluation of Holstein final score. Journal of Dairy Science 93: 743–752. https://doi.org/10.3168/jds.2009-2730

Araus J. L., S. C. Kefauver, M. Zaman-Allah, M. S. Olsen, and J. E. Cairns, 2018 Translating high-throughput phenotyping into genetic gain. Trends in Plant Science 23: 451–466. https://doi.org/10.1016/j.tplants.2018.02.001

Bartholomé J., J. Van Heerwaarden, F. Isik, C. Boury, M. Vidal, *et al.*, 2016 Performance of genomic prediction within and across generations in maritime pine. BMC Genomics 17: 604. https://doi.org/10.1186/s12864-016-2879-8

Beaulieu J., T. K. Doerksen, J. MacKay, A. Rainville, and J. Bousquet, 2014 Genomic selection accuracies within and between environments and small breeding groups in white spruce. BMC Genomics 15: 1048. https://doi.org/10.1186/1471-2164-15-1048

Bian L., J. Shi, R. Zheng, J. Chen, and H. X. Wu, 2014 Genetic parameters and genotype–environment interactions of Chinese fir (*Cunninghamia lanceolata*) in Fujian Province. Can. J. For. Res. 44: 582–592. https://doi.org/10.1139/cjfr-2013-0427

Burdon R. D., 1977 Genetic correlation as a concept for studying genotype-environment interaction in forest tree breeding. Silvae Genetica 26: 168–175.

Butler D. G., A. R. Gilmour, and B. J. Gogel, 2009 ASReml-R reference manual

618 Campbell R. K., 1992 Genotype * environment interaction: a case study for Douglas-fir in
619 western Oregon. Res. Pap. PNW-RP-455. Portland, OR: US Department of Agriculture,
620 Forest Service, Pacific Northwest Research Station. 21 p 455.

621 Cappa E. P., A. D. Yanchuk, and C. V. Cartwright, 2012 Bayesian inference for multi-
622 environment spatial individual-tree models with additive and full-sib family genetic
623 effects for large forest genetic trials. Annals of Forest Science 69: 627–640.
624 https://doi.org/10.1007/s13595-011-0179-7

625 Cappa E. P., M. U. Stoehr, C.-Y. Xie, and A. D. Yanchuk, 2016 Identification and joint
626 modeling of competition effects and environmental heterogeneity in three Douglas-fir
627 (*Pseudotsuga menziesii* var. menziesii) trials. Tree Genetics & Genomes 12: 102.
628 https://doi.org/10.1007/s11295-016-1061-4

629 Cappa E. P., Y. A. El-Kassaby, F. Muñoz, M. N. Garcia, P. V. Villalba, *et al.*, 2018 Genomic-
630 based multiple-trait evaluation in Eucalyptus grandis using dominant DArT markers.
631 Plant Science 271: 27–33. https://doi.org/10.1016/j.plantsci.2018.03.014

632 Chen Z.-Q., J. Baison, J. Pan, B. Karlsson, B. Andersson, *et al.*, 2018 Accuracy of genomic
633 selection for growth and wood quality traits in two control-pollinated progeny trials using
634 exome capture as the genotyping platform in Norway spruce. BMC Genomics 19: 946.
635 https://doi.org/10.1186/s12864-018-5256-y

636 Christensen O. F., and M. S. Lund, 2010 Genomic prediction when some animals are not
637 genotyped. Genetics Selection Evolution 42: 2. https://doi.org/10.1186/1297-9686-42-2

638 Christensen O. F., P. Madsen, B. Nielsen, T. Ostersen, and G. Su, 2012 Single-step methods for
639 genomic evaluation in pigs. animal 6: 1565–1571.
640 https://doi.org/10.1017/S1751731112000742

641 Danecek P., A. Auton, G. Abecasis, C. A. Albers, E. Banks, *et al.*, 2011 The variant call format
642 and VCFtools. Bioinformatics 27: 2156–2158.
643 https://doi.org/10.1093/bioinformatics/btr330

644 Dungey H. S., J. P. Dash, D. Pont, P. W. Clinton, M. S. Watt, *et al.*, 2018 Phenotyping whole
645 forests will help to track genetic performance. Trends in Plant Science 23: 854–864.
646 https://doi.org/10.1016/j.tplants.2018.08.005

647 Gamal El-Dien O., B. Ratcliffe, J. Klápště, C. Chen, I. Porth, *et al.*, 2015 Prediction accuracies
648 for growth and wood attributes of interior spruce in space using genotyping-by-
649 sequencing. BMC Genomics 16: 370. https://doi.org/10.1186/s12864-015-1597-y

650 Gilmour A. R., R. Thompson, and B. R. Cullis, 1995 Average Information REML: An efficient
651 algorithm for variance parameter estimation in linear mixed models. Biometrics 51:
652 1440–1450. https://doi.org/10.2307/2533274

653 Grattapaglia D., 2017 Status and perspectives of genomic selection in forest tree breeding, pp.
654 199–249 in *Genomic Selection for Crop Improvement: New Molecular Breeding*
655 *Strategies for Crop Improvement*, edited by Varshney R. K., Roorkiwal M., Sorrells M.
656 E. Springer International Publishing, Cham.

657 Grattapaglia D., O. B. Silva-Junior, R. T. Resende, E. P. Cappa, B. S. de F. Müller, *et al.*, 2018
658 Quantitative genetics and genomics converge to accelerate forest tree breeding. Front.
659 Plant Sci. 9. https://doi.org/10.3389/fpls.2018.01693

660 Hayes B. J., P. J. Bowman, A. J. Chamberlain, and M. E. Goddard, 2009 Invited review:
661 Genomic selection in dairy cattle: Progress and challenges. Journal of Dairy Science 92:
662 433–443. https://doi.org/10.3168/jds.2008-1646

663 Isik F., J. Bartholomé, A. Farjat, E. Chancerel, A. Raffin, *et al.*, 2016 Genomic selection in
664 maritime pine. Plant Science 242: 108–119.
665 https://doi.org/10.1016/j.plantsci.2015.08.006

666 Isik F., J. Holland, and C. Maltecca, 2017 *Genetic Data Analysis for Plant and Animal Breeding*.
667 Springer International Publishing.

668 Jarquín D., J. Crossa, X. Lacaze, P. Du Cheyron, J. Daucourt, *et al.*, 2014 A reaction norm model
669 for genomic selection using high-dimensional genomic and environmental data. Theor
670 Appl Genet 127: 595–607. https://doi.org/10.1007/s00122-013-2243-1

671 Klápště J., M. Suontama, H. S. Dungey, E. J. Telfer, N. J. Graham, *et al.*, 2018 Effect of hidden
672 relatedness on single-step genetic evaluation in an advanced open-pollinated breeding
673 program. J Hered 109: 802–810. https://doi.org/10.1093/jhered/esy051

674 Legarra A., I. Aguilar, and I. Misztal, 2009 A relationship matrix including full pedigree and
675 genomic information. Journal of Dairy Science 92: 4656–4663.
676 https://doi.org/10.3168/jds.2009-2061

677 Legarra A., and V. Ducrocq, 2012 Computational strategies for national integration of
678 phenotypic, genomic, and pedigree data in a single-step best linear unbiased prediction.
679 Journal of Dairy Science 95: 4629–4645. https://doi.org/10.3168/jds.2011-4982

680 Lenz P. R. N., J. Beaulieu, S. D. Mansfield, S. Clément, M. Desponts, *et al.*, 2017 Factors
681 affecting the accuracy of genomic selection for growth and wood quality traits in an
682 advanced-breeding population of black spruce (*Picea mariana*). BMC Genomics 18: 335.
683 https://doi.org/10.1186/s12864-017-3715-5

684 Li Y., M. Suontama, R. D. Burdon, and H. S. Dungey, 2017 Genotype by environment
685 interactions in forest tree breeding: review of methodology and perspectives on research
686 and application. Tree Genetics & Genomes 13: 60. https://doi.org/10.1007/s11295-017-
687 1144-x

688 Lourenco D. a. L., S. Tsuruta, B. O. Fragomeni, Y. Masuda, I. Aguilar, *et al.*, 2015 Genetic
689 evaluation using single-step genomic best linear unbiased predictor in American Angus. J
690 Anim Sci 93: 2653–2662. https://doi.org/10.2527/jas.2014-8836

691 Marchal A., C. D. Schlichting, R. Gobin, P. Balandier, F. Millier, *et al.*, 2019 Deciphering hybrid
692 larch reaction norms using random regression. G3: Genes, Genomes, Genetics 9: 21–32.
693 https://doi.org/10.1534/g3.118.200697

694 Meuwissen T. H. E., B. J. Hayes, and M. E. Goddard, 2001 Prediction of total genetic value
695 using genome-wide dense marker maps. Genetics 157: 1819–1829.

696 Misztal I., A. Legarra, and I. Aguilar, 2009 Computing procedures for genetic evaluation
697 including phenotypic, full pedigree, and genomic information. Journal of Dairy Science
698 92: 4648–4655. https://doi.org/10.3168/jds.2009-2064

699 Morais Júnior O. P., J. B. Duarte, F. Breseghello, A. S. G. Coelho, O. P. Morais, *et al.*, 2018
700 Single-step reaction norm models for genomic prediction in multienvironment recurrent
701 selection trials. Crop Science 58: 592–607. https://doi.org/10.2135/cropsci2017.06.0366

702 Pérez P., and G. de los Campos, 2014 Genome-wide regression and prediction with the BGLR
703 statistical package. Genetics 198: 483–495. https://doi.org/10.1534/genetics.114.164442

704 Pérez-Rodríguez P., J. Crossa, K. Bondalapati, G. De Meyer, F. Pita, *et al.*, 2015 A pedigree-
705 based reaction norm model for prediction of cotton yield in multienvironment trials. Crop
706 Science 55: 1143–1151. https://doi.org/10.2135/cropsci2014.08.0577

707 Perry P. O., 2015 *bcv: Cross-validation for the SVD (Bi-Cross-Validation)*. R package version
708 1.0.1.

709 Ratcliffe B., O. G. El-Dien, E. P. Cappa, I. Porth, J. Klápště, *et al.*, 2017 Single-step BLUP with
710 varying genotyping effort in open-pollinated *Picea glauca*. G3: Genes, Genomes,
711 Genetics 7: 935–942. https://doi.org/10.1534/g3.116.037895

712 Resende M. F. R., P. Muñoz, J. J. Acosta, G. F. Peter, J. M. Davis, *et al.*, 2012 Accelerating the
713 domestication of trees using genomic selection: Accuracy of prediction models across
714 ages and environments. New Phytologist 193: 617–624. https://doi.org/10.1111/j.1469-
715 8137.2011.03895.x

716 Resende R. T., M. D. V. Resende, F. F. Silva, C. F. Azevedo, E. K. Takahashi, *et al.*, 2017
717 Regional heritability mapping and genome-wide association identify loci for complex
718 growth, wood and disease resistance traits in Eucalyptus. New Phytologist 213: 1287–
719 1300. https://doi.org/10.1111/nph.14266

720 Silva J. C. e, G. W. Dutkowski, and N. M. G. Borralho, 2005 Across-site heterogeneity of
721 genetic and environmental variances in the genetic evaluation of *Eucalyptus globulus*
722 trials for height growth. Ann. For. Sci. 62: 183–191.
723 https://doi.org/10.1051/forest:2005010

724 Spiegelhalter D. J., N. G. Best, B. P. Carlin, and A. V. D. Linde, 2002 Bayesian measures of
725 model complexity and fit. Journal of the Royal Statistical Society: Series B (Statistical
726 Methodology) 64: 583–639. https://doi.org/10.1111/1467-9868.00353

727 Stackhouse P. W. J., D. Westberg, W. S. Chandler, T. Zhang, and J. M. Hoell, 2017 *Prediction*
728 *Of Worldwide Energy Resource (POWER)---Agroclimatology Methodology---(1.0 o*
729 *Latitude by 1.0 o Longitude Spatial Resolution)*. NASA, NASA Langley Research
730 Center, SSAI/NASA Langley Research Center.

731 Stejskal J., M. Lstibůrek, J. Klápště, J. Čepl, and Y. A. El-Kassaby, 2018 Effect of genomic
732 prediction on response to selection in forest tree breeding. Tree Genetics & Genomes 14:
733 74. https://doi.org/10.1007/s11295-018-1283-8

734 Tan B., D. Grattapaglia, G. S. Martins, K. Z. Ferreira, B. Sundberg, *et al.*, 2017 Evaluating the
735 accuracy of genomic prediction of growth and wood traits in two Eucalyptus species and

their F1 hybrids. BMC Plant Biology 17: 110. https://doi.org/10.1186/s12870-017-1059-6

Thistlethwaite F. R., B. Ratcliffe, J. Klápště, I. Porth, C. Chen, *et al.*, 2017 Genomic prediction accuracies in space and time for height and wood density of Douglas-fir using exome capture as the genotyping platform. BMC Genomics 18: 930. https://doi.org/10.1186/s12864-017-4258-5

Thistlethwaite F. R., B. Ratcliffe, J. Klápště, I. Porth, C. Chen, *et al.*, 2019 Genomic selection of juvenile height across a single-generational gap in Douglas-fir. Heredity https://doi.org/10.1038/s41437-018-0172-0

VanRaden P. M., 2008 Efficient methods to compute genomic predictions. Journal of Dairy Science 91: 4414–4423. https://doi.org/10.3168/jds.2007-0980

VanRaden P. M., C. P. Van Tassell, G. R. Wiggans, T. S. Sonstegard, R. D. Schnabel, *et al.*, 2009 Invited Review: Reliability of genomic predictions for North American Holstein bulls. Journal of Dairy Science 92: 16–24. https://doi.org/10.3168/jds.2008-1514

Vitezica Z. G., I. Aguilar, I. Misztal, and A. Legarra, 2011 Bias in genomic predictions for populations under selection. Genetics Research 93: 357–366. https://doi.org/10.1017/S001667231100022X

Wang H., I. Misztal, I. Aguilar, A. Legarra, and W. M. Muir, 2012a Genome-wide association mapping including phenotypes from relatives without genotypes. Genetics Research 94: 73–83. https://doi.org/10.1017/S0016672312000274

Wang T., A. Hamann, D. L. Spittlehouse, and T. Q. Murdock, 2012b ClimateWNA - High-resolution spatial climate data for western North America. J. Appl. Meteor. Climatol. 51: 16–29. https://doi.org/10.1175/JAMC-D-11-043.1

FIGURES

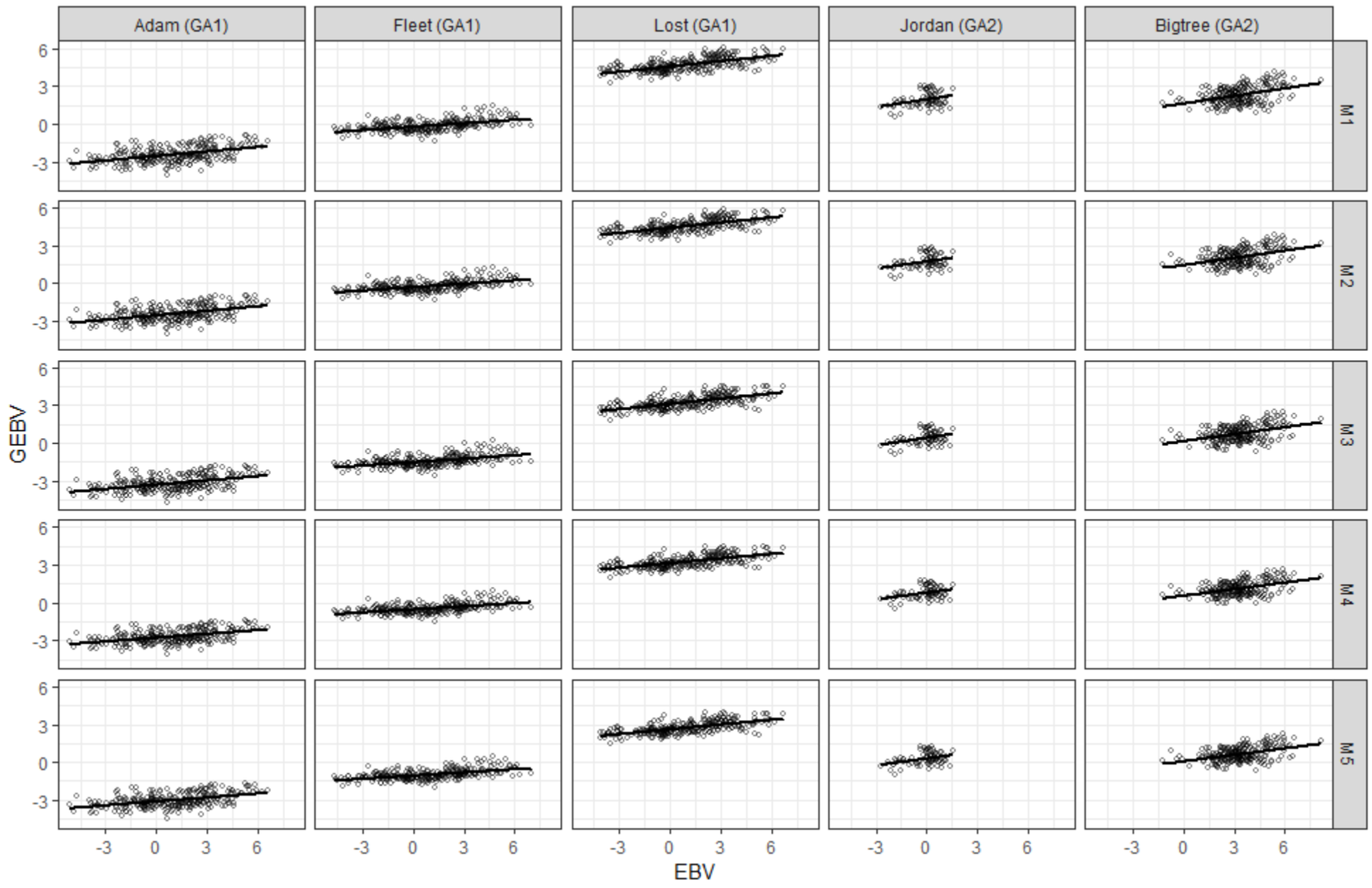

Figure 1: Scatterplots of intra-generation (GA1) and inter-generation (GA2) predictions of EBV.

TABLES

Table 1: Experimental population summaries for pedigree-based analyses.

Environment	N_{tree}	N_{Par}	N_{FSFam}	Age	Latitude	Longitude	Elevation (mas)	Date
			Parents (F1)					
Lost	2,464	78	165	12	49° 22′ 15″	122° 14′ 07″	424	1975-1987
Adam	2,368	78	165	12	50° 24′ 42”	126° 09′ 37″	576	1975-1987
Fleet	2,595	78	165	12	48° 39′ 25″	128° 05′ 05″	561	1975-1987
Sechelt	2,472	78	165	12	49° 28' 05"	123° 42' 00"	227	1975-1987
Eldred	2,389	78	165	12	50° 08' 51"	124° 11' 19"	148	1975-1987
Menzies	2,509	78	165	12	50° 08' 55"	125° 38' 16"	333	1975-1987
Sproat	2,485	78	165	12	49° 17' 44"	125° 03' 10"	318	1975-1987
Squamish	2,477	78	165	12	50° 11' 51"	123° 22' 40"	470	1975-1987
Tansky	2,607	78	165	12	48° 27' 52"	124° 01' 48"	545	1975-1987
White	2,503	78	165	12	50° 06' 03"	126° 04' 54"	409	1975-1987
			Series 2 (F2-2)					
Jordan	1,551	74	79	11	48° 25’ 86"	124° 01’ 80"	160	2003-2014
North Arm	1,583	75	81	11	48° 50’ 72"	124° 06’ 53"	168	2003-2014
			Series 3 (F2-3)					
Big Tree	2,228	73	108	11	50° 15’ 80"	125° 43’ 59"	225	2006-2017
Roach	1,768	73	104	11	48° 45’ 08"	124° 06' 14"	230	2006-2017

NOTE: N_{tree}, Number of individual tree observations; N_{Par}, Combined number of male and female parents; N_{FSFam}, Number of full-sibling families; Age, Age of tree height measurement; Date, Year of planting to year of tree height measurement.

Table 2: Training (T) and validation (V) population summaries for genomic analyses.

Environment	Generation	N_{Tree}	N_{Par}	N_{FSFam}	$N_{Genotyped}$	GA1	GA2
Lost	F1	1,167	36	78	288	T / V	T
Adam	F1	1,114	36	78	285	T / V	T
Fleet	F1	1,228	36	78	295	T / V	T
Sechelt	F1	1,164	36	78	-	T	T
Eldred	F1	1,130	36	78	-	T	T
Menzies	F1	1,191	36	78	-	T	T
Sproat	F1	1,170	36	78	-	T	T
Squamish	F1	1,169	36	78	-	T	T
Tansky	F1	1,236	36	78	-	T	T
White	F1	1,190	36	78	-	T	T
Jordan	F2-2	171	9	8	79	-	V
Bigtree	F2-3	821	26	41	230	-	V

NOTE: GA1, Genomic Analysis 1; GA2, Genomic Analysis 2; T, training population; V, validation population; N_{Tree}, Number of individual tree observations; N_{Par}, Combined number of male and female parents; N_{FSFam}, Number of full-sibling families.

Table 3: Pedigree based single environment narrow-sense heritabilities (diagonal) and Type-B genetic correlations (lower triangle) for MAI, standard errors in parentheses.

	Lost	Adam	Fleet	Sechelt	White	Menzies	Sproat	Tansky	Eldred	Squamish	Bigtree	Roach	Jordan	Northarm
Lost	**0.13 (0.002)**													
Adam	0.71 (0.128)	**0.18 (0.002)**												
Fleet	0.83 (0.131)	0.88 (0.089)	**0.22 (0.004)**											
Sechelt	b	0.77 (0.097)	0.98 (0.071)	**0.22 (0.003)**										
White	0.73 (0.138)	0.85 (0.100)	0.93 (0.078)	0.93 (0.078)	**0.04 (0.014)**									
Menzies	0.83 (0.137)	0.90 (0.095)	0.92 (0.117)	0.91 (0.099)	0.97 (0.097)	**0.17 (0.003)**								
Sproat	0.55 (0.163)	0.51 (0.142)	0.78 (0.116)	0.80 (0.104)	0.78 (0.115)	0.81 (0.128)	**0.21 (0.003)**							
Tansky	0.73 (0.138)	0.63 (0.121)	0.89 (0.083)	0.84 (0.090)	0.67 (0.125)	0.72 (0.132)	0.60 (0.136)	**0.27 (0.005)**						
Eldred	0.77 (0.159)	0.61 (0.148)	0.77 (0.144)	0.98 (0.100)	0.91 (0.108)	0.89 (0.139)	0.86 (0.139)	0.72 (0.148)	**0.14 (0.002)**					
Squamish	0.83 (0.103)	0.85 (0.068)	0.87 (0.076)	0.84 (0.080)	0.80 (0.090)	0.93 (0.070)	0.62 (0.120)	0.64 (0.120)	0.70 (0.135)	**0.25 (0.002)**				
Bigtree	-0.23 (0.604)	-0.01 (0.474)	0.53 (0.394)	-0.14 (0.472)	0.09 (0.529)	0.13 (0.597)	-0.53 (0.455)	-0.04 (0.554)	-0.06 (0.575)	-0.05 (0.565)	**0.13 (0.000)**			
Roach	0.48 (0.468)	0.46 (0.368)	0.32 (0.418)	0.31 (0.407)	0.20 (0.471)	0.51 (0.452)	-0.03 (0.506)	0.24 (0.480)	0.19 (0.500)	0.70 (0.338)	0.57 (0.133)	**0.33 (0.000)**		
Jordan	0.73 (0.488)	0.64 (0.430)	0.20 (0.504)	0.72 (0.400)	0.80 (0.540)	b	0.98 (0.369)	0.41 (0.573)	b	0.35 (0.455)	b	b	**0.42 (0.006)**	
Northarm	b	b	b	0.89 (0.430)	b	b	b	b	b	0.75 (0.435)	b	b	0.62 (0.194)	**0.12 (0.003)**

NOTE: b, Type-B genetic correlation and their approximate standard errors were not estimated due to convergence problems.

Table 4: Model Deviance Information Criterion (DIC), posterior means and their 95% highest posterior density (HPD) intervals in brackets for the additive variance ($\hat{\sigma}_a^2$), replicate within environment variance ($\hat{\sigma}_r^2$), environmental variance ($\hat{\sigma}_s^2$), environment covariates variance ($\hat{\sigma}_w^2$), the interaction between additive effects and environment covariates ($\hat{\sigma}_{aw}^2$), the variance of the interaction between additive and environmental effects ($\hat{\sigma}_{as}^2$), residual variance ($\hat{\sigma}_e^2$), heritability ($\hat{h}^2$). See text for models´ abbreviations.

Model	DIC	$\hat{\sigma}_a^2$	$\hat{\sigma}_r^2$	$\hat{\sigma}_s^2$	$\hat{\sigma}_w^2$	$\hat{\sigma}_{aw}^2$	$\hat{\sigma}_{as}^2$	$\hat{\sigma}_e^2$	$\hat{h}^2$
M1	87846.80	20.02 [13.00 27.59]	11.11 [6.35 16.63]	102.53 [38.18 193.00]	- -	- -	- -	91.35 [86.24 96.17]	0.18 [0.12 0.24]
M2	87850.41	19.11 [12.58 26.08]	9.20 [5.27 14.01]	90.52 [24.32 186.18]	58.04 [10.15 181.48]	- -	- -	91.55 [86.67 96.23]	0.17 [0.12 0.23]
M3	87176.25	18.51 [11.89 25.15]	8.05 [4.65 12.22]	86.16 [26.04 168.63]	33.86 [8.22 70.70]	19.99 [14.88 25.31]	- -	76.61 [71.10 82.19]	0.16 [0.11 0.21]
M4	87380.72	17.41 [11.27 23.88]	8.03 [4.57 12.32]	85.50 [21.92 172.05]	38.95 [8.84 99.37]	- -	12.82 [9.67 15.94]	81.12 [76.17 86.00]	0.16 [0.10 0.21]
M5	87159.53	16.53 [10.87 22.92]	7.20 [4.07 10.97]	90.08 [25.45 181.30]	30.08 [5.37 65.72]	12.19 [6.96 17.48]	8.52 [5.64 11.49]	76.43 [71.27 81.92]	0.15 [0.10 0.20]

Table 5: Intra-generation (GA1) cross-validation prediction accuracies ($r_{(GEBV,EBV)}$) with standard errors (SE). See text for models´ abbreviations.

	Lost		Adam		Fleet	
	$r_{(GEBV,EBV)}$	SE	$r_{(GEBV,EBV)}$	SE	$r_{(GEBV,EBV)}$	SE
M1	0.601	0.0000	0.447	0.0004	0.498	0.0006
M2	0.613	0.0011	0.453	0.0011	0.513	0.0027
M3	0.640	0.0007	0.461	0.0006	0.519	0.0010
M4	0.615	0.0011	0.448	0.0010	0.515	0.0010
M5	0.629	0.0009	0.452	0.0010	0.526	0.0023

Table 6: Inter-generation (GA2) cross-validation prediction accuracies ($r_{(GEBV,EBV)}$) and standard errors (SE). See text for models´ abbreviations.

	Jordan		Bigtree	
	$r_{(GEBV,EBV)}$	SE	$r_{(GEBV,EBV)}$	SE
M1	0.320	0.0012	0.506	0.0006
M2	0.317	0.0011	0.506	0.0008
M3	0.360	0.0015	0.535	0.0009
M4	0.346	0.0029	0.526	0.0006
M5	0.360	0.0016	0.538	0.0004

SUPPLEMENTS

Figure S1: Three generation coastal Douglas-fir contemporary pedigree containing the inter-generation validation population of study. Circles represent single individuals; octagons represent full-sibling families. Red colours are the unrelated (assumed) base population of wild plus tree selections (P0), green colours are the forward selection progenitors (F1) of the Jordan (purple, F2-2) and Bigtree (yellow, F2-3) validation populations (F2) respectively. The pedigree was produced using Helium software (Shaw *et al.*, 2014).

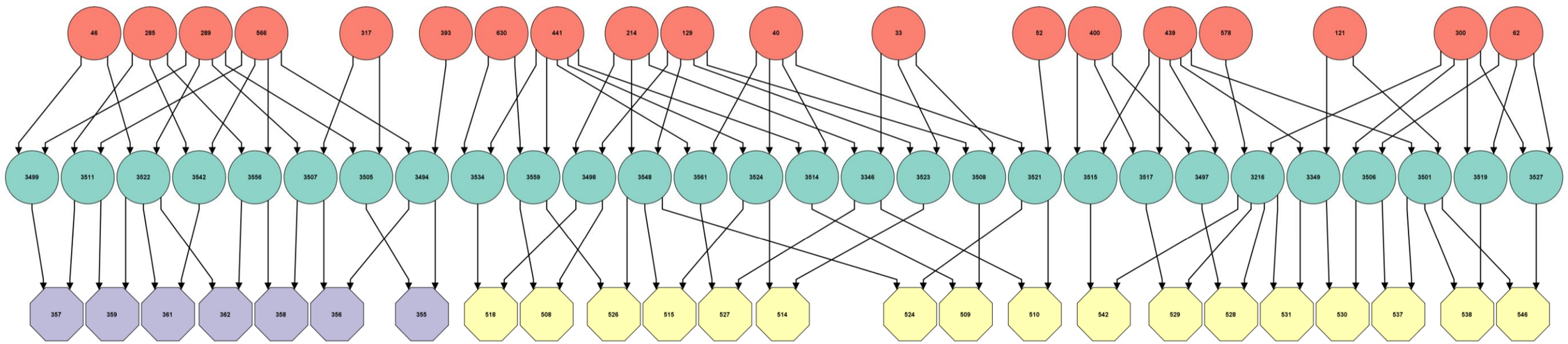

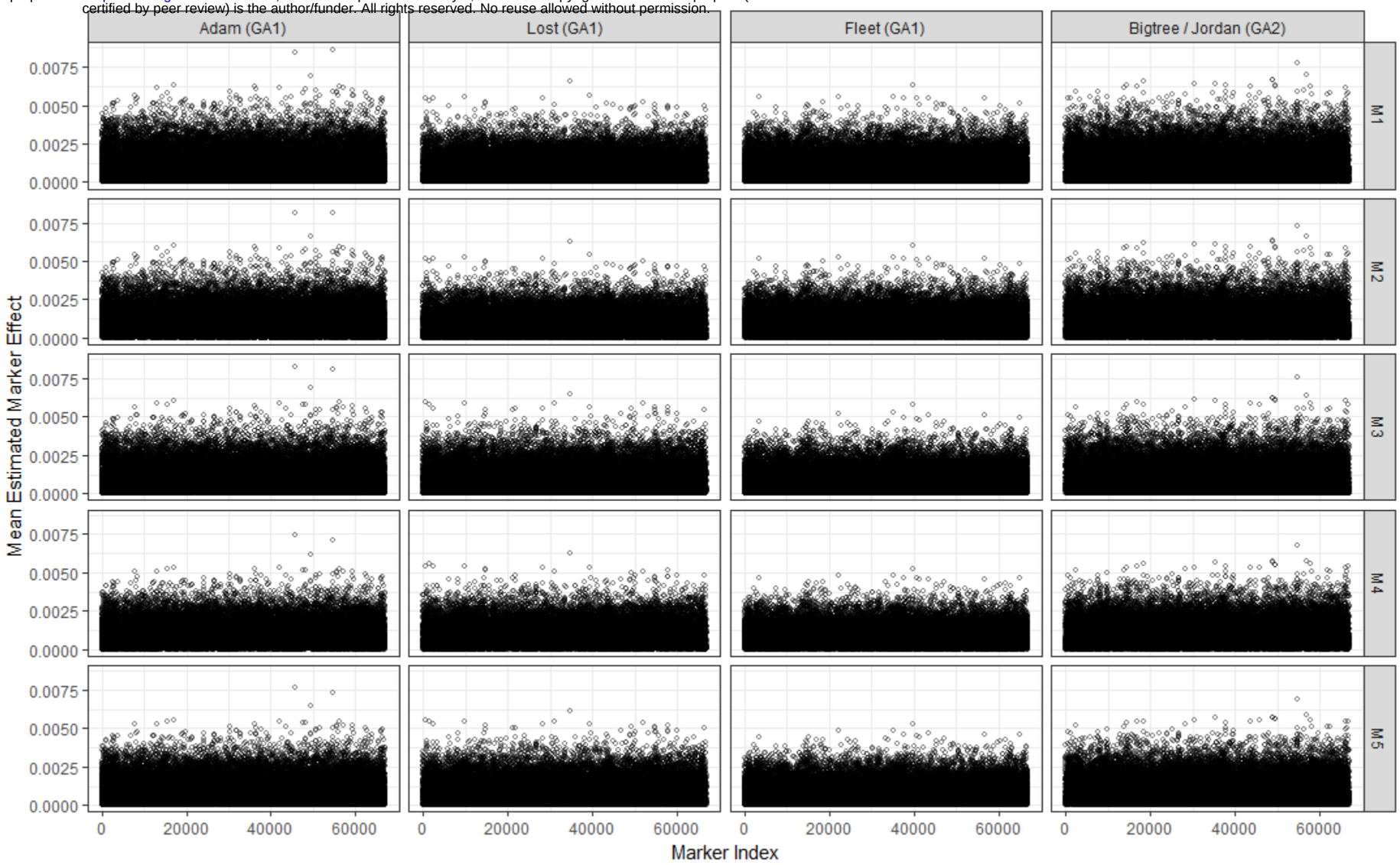

Figure S2: Scatterplot of mean absolute marker effects from the cross-validation analysis.

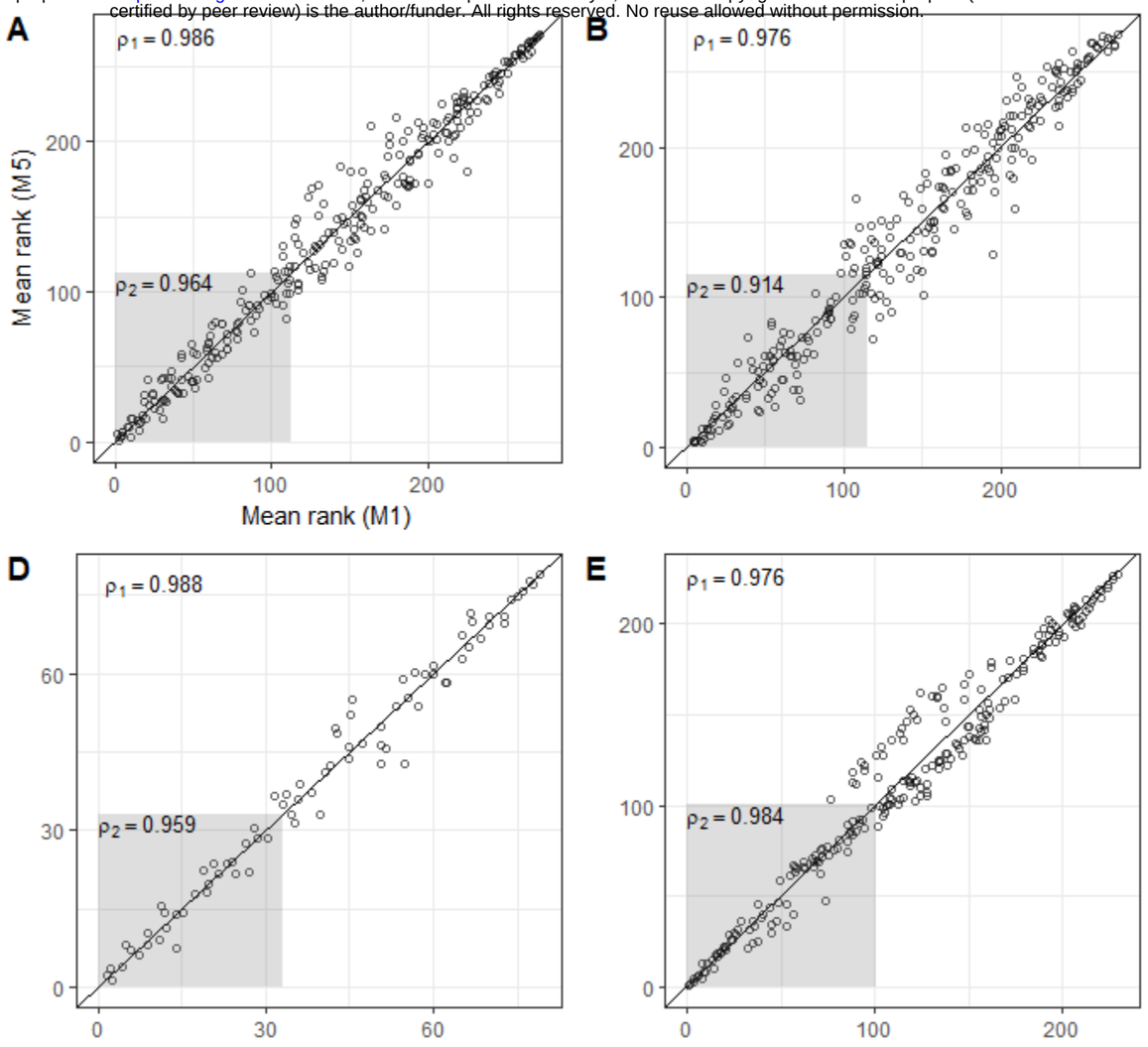

Figure S3: Scatterplots of mean rank of predicted trees with Spearman rank correlation coefficients from the cross-validation analyses for all predictions (ρ_1) and top 40% of predictions (ρ_2) within environments Adam (A), Lost (B), Fleet (C), Jordan (D), and Bigtree (E) comparing the base model (M1, x-axis) and fully specified model (M5, y-axis). Deviation from the diagonal line implies a rank change.

Table S1: Number of parent-parent (F1-F1 / F2-F2) or parent-grandparent (F1-F2) (above diagonal) and families (below diagonal) in common among the environments for study population 1 (SP1).

Generation		F1										F2-2		F2-3	
		Lost	Adam	Fleet	Sechelt	Eldred	Menzies	Sproat	Squamish	Tansky	White	Jordan	Northarm	Bigtree	Roach
F1	Lost		78	78	78	78	78	78	78	78	78	13	13	12	12
	Adam	165		78	78	78	78	78	78	78	78	13	13	12	12
	Fleet	165	165		78	78	78	78	78	78	78	13	13	12	12
	Sechelt	165	165	165		78	78	78	78	78	78	13	13	12	12
	Eldred	165	165	165	165		78	78	78	78	78	13	13	12	12
	Menzies	165	165	165	165	165		78	78	78	78	13	13	12	12
	Sproat	165	165	165	165	165	165		78	78	78	13	13	12	12
	Squamish	165	165	165	165	165	165	165		78	78	13	13	12	12
	Tansky	165	165	165	165	165	165	165	165		78	13	13	12	12
	White	165	165	165	165	165	165	165	165	165		13	13	12	12
F2-2	Jordan												74		
	Northarm											79			
	Bigtree														73
F2-3	Roach													104	

Table S2: Number of F2 parents within the F1 environments.

		F2-2		F2-3	
		Jordan	Northarm	Bigtree	Roach
F1	Lost	4	4	5	5
	Adam	6	6	4	4
	Fleet	7	7	8	8
	Sechelt	8	8	9	9
	Eldred				
	Menzies				
	Sproat				
	Squamish				
	Tansky				
	White				

Table S3: List of monthly (from January/01 to December/12) climatic variables obtained from ClimateBC v5.51 (Wang *et al.*, 2012a) used in the genomic analyses.

Primary monthly variables	
Tave01 – Tave12	mean temperatures (°C)
TMX01 – TMX12	maximum mean temperatures (°C)
TMN01 – TMN12	minimum mean temperatures (°C)
PPT01 – PPT12	precipitation (mm)
RAD01 – RAD12	solar radiation (MJ m^{-2} d^{-1})
Derived monthly variables	
DD_0_01 – DD_0_12	degree-days below 0°C
DD5_01 – DD5_12	degree-days above 5°C
DD_18_01 – DD_18_12	degree-days below 18°C
DD18_01 – DD18_12	degree-days above 18°C
NFFD01 – NFFD12	number of frost-free days
PAS01 – PAS12	precipitation as snow (mm)
Eref01 – Eref12	Hargreaves reference evaporation (mm)
CMD01 – CMD12	Hargreaves climatic moisture deficit (mm)